

BEAM INJECTOR AND TRANSPORT CALCULATIONS FOR ITS

Thomas P. Hughes, Mission Research Corporation, Albuquerque, NM 87106
David C. Moir and Paul W. Allison, Los Alamos National Laboratory, Los Alamos, NM 87545

Abstract

The Integrated Test Stand at Los Alamos National Laboratory (LANL) is addressing issues in high-brightness electron beam generation, acceleration, and transport. The machine consists of a 3 kA, 3.5 MV injector, eight induction acceleration gaps, a drift section and a final-focus magnet which focuses the beam onto diagnostic targets. One of the goals of the program is to test and improve the predictive capability of numerical models. We have carried out detailed simulations of the diode and initial drift region with the particle-in-cell codes IVORY and SPROP, obtaining good agreement with experimental streak-camera data at several axial locations. Transport through the accelerating cells to the target 10 m from the cathode is modeled with the envelope codes LAMDA and XTR. The magnet settings for minimum spot-size are close to the experimental values. From the measured value of the minimum spot-size we infer a normalized Lapostolle emittance of about 0.2 cm-rad. We have characterized the sensitivity of the spot-size to variation in the machine parameters.

I. INJECTOR SIMULATIONS

The standard injector geometry in the ITS has a 18 cm AK gap and a flat 3" diameter velvet emitting surface (Fig. 1). This surface is indented by 2 mm from the surrounding flat electrode. The small scale of this indentation means that a fine mesh is needed to simulate the AK gap. We used the particle-in-cell simulation code IVORY and the iterative trajectory code PBGUNS [1] to model the injector. The codes agree well with each other and with the experimental beam current measurement (3 kA at 3.5 MV), as shown in Fig. 2. The effect of the indentation is to reduce the current density at the beam edge, and provide some radial focusing to the emitted beam. With a previous flush emitting surface, we were unable to get close agreement between experiment and simulation [2]. The measured emission current was about 15% higher than the calculation, and current was lost to the anode even when the extraction field was relatively high. We believe that this was due to poorly understood effects at the edge of the velvet emitter which produced low quality, divergent emission in this region.

The simulation in Fig. 1 had no intrinsic emittance at the cathode. Such emittance, inferred from spot-size measurements discussed below, can easily be added to the simulation as an effective transverse temperature of the emitted particles. For the large beam radii in Fig. 1, the transport is space-charge dominated.

II. RADIAL CURRENT PROFILE COMPARISONS IN PRE-ACCELERATOR DRIFT

A series of measurements of the beam radial current density profile was made by placing a quartz fiber across the beam diameter to generate Cherenkov light. The light was imaged with

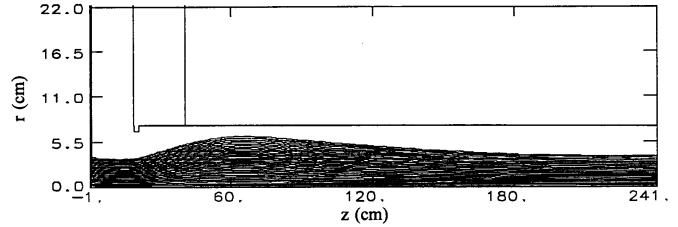


Figure 1. Beam particle positions for IVORY simulation of ITS indented cathode. Mesh is $\Delta z \times \Delta r = 0.1 \text{ cm} \times 0.1 \text{ cm}$ in AK gap, and $0.4 \text{ cm} \times 0.2 \text{ cm}$ for $z > 40 \text{ cm}$. ($I_b = 3 \text{ kA}$, $V_b = 3.48 \text{ MV}$, anode magnet current = 175 A).

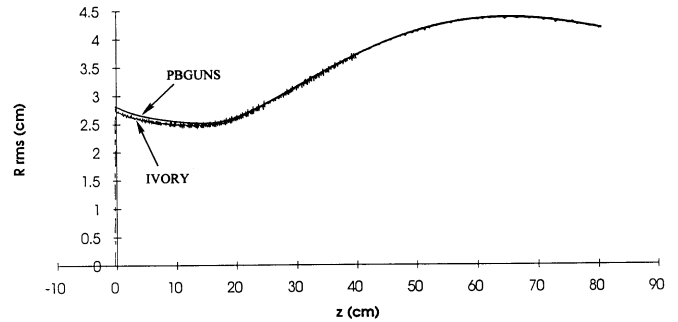


Figure 2. Comparison of r.m.s. beam radius from IVORY simulation and PBGUNS simulation of ITS cathode with 2 mm indentation. Emitted current for both simulations is 3 kA at 3.48 MV.

a streak camera to get a time-resolved measurement. To simulate beam transport from the diode to the location of these measurements (about 2 m from the cathode surface), we developed a beam slice code SPROP [3]. The field equations for this code are obtained from the full Maxwell equations by setting axial derivatives to zero and solving the resulting equations on a 1-D radial mesh using Fourier transforms in the azimuthal direction. The code is initialized with particles from an IVORY simulation at 101 cm from the cathode surface, which is in the downstream fringe-field of the anode magnet. Comparisons with the experiment were made at 170, 192 and 212 cm from the cathode electrode. The results at $z = 212 \text{ cm}$, shown in Fig. 3, are typical of the good agreement obtained. The result in Fig. 3(b) is about 60 cm downstream of where the beam focuses to a small ($\approx 0.5 \text{ cm}$ radius) spot.

III. BEAM RADIUS MEASUREMENTS AT FINAL FOCUS

The ITS injector is followed by eight ferrite induction accelerating cells which typically have voltages of 200–250 kV per gap. The beam then goes into a drift section which has an intermediate

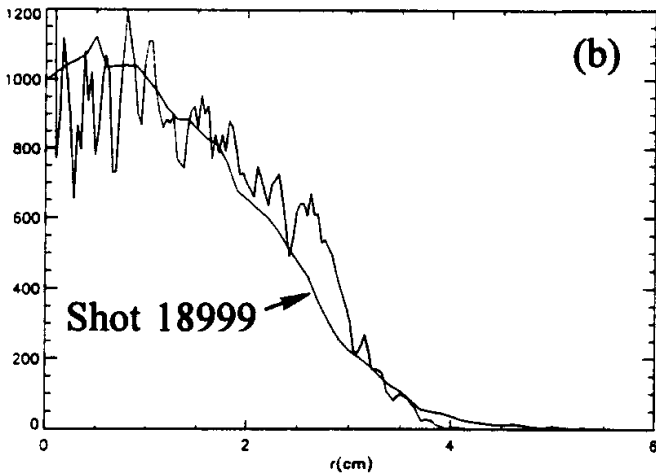
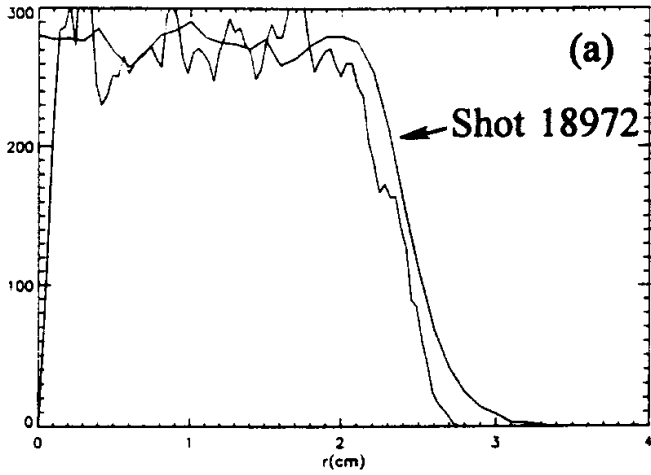


Figure 3. Comparison of experimental and numerical radial current density profiles at 212 cm from the cathode for anode magnet currents of (a) 185 A and (b) 210 A. Vertical scale is arbitrary.

focusing solenoid and a final focus solenoid (FFS). The purpose of the drift section is to prevent shrapnel from fragmented targets from damaging the acceleration cells. A rotating shutter is also used for this purpose.

Since the ITS is directed at radiographic applications requiring small beam spot-size, the principal diagnostic technique consists of measuring the radius of the focal spot as a function of FFS strength. We can model the entire transport using SPROP, but for speed we generally employ the envelope codes LAMDA [4] and XTR [5]. We have found that the effect of beam rotation in the focusing solenoids is non-negligible. Starting from exact laminar beam equilibria obtained by Reiser [6], a modified envelope equation was obtained to take account of this effect [3]. The envelope equation, which assumes constant emittance, closely matches SPROP, as shown in Fig. 4. The SPROP simulations show that in fact there is little emittance variation through the accelerator.

A comparison between the spot-size measurements at $z = 10$ m and LAMDA for a particular tune is shown in Fig. 5. The LAMDA beam envelope for the minimum spot-size is shown in

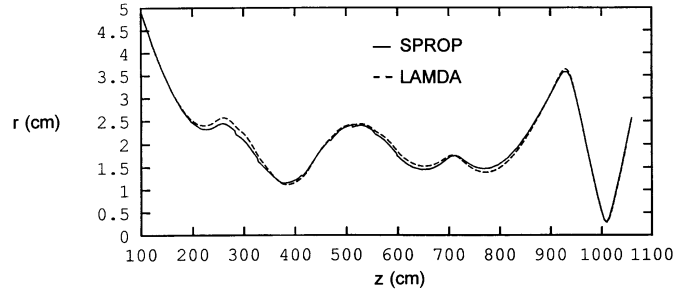


Figure 4. Comparison of envelope obtained from SPROP particle-in-cell simulation with LAMDA envelope simulation

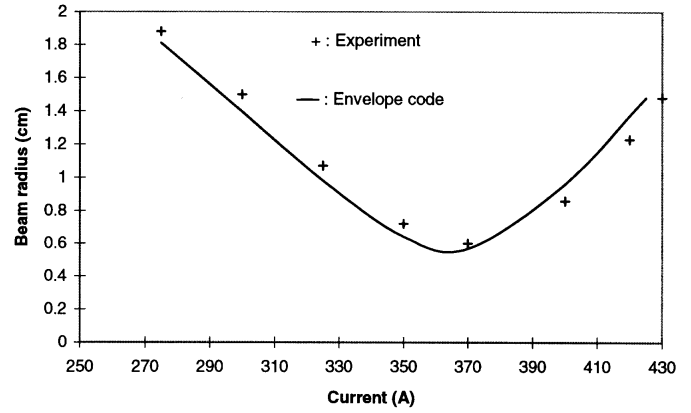


Figure 5. Beam radius at final focus as a function of final-focus solenoid current, comparing measurements with envelope code predictions. Experimental results are averaged over 60 ns flat-top.

Fig. 6. Based on this and other comparisons for different magnet tunes, we deduce a normalized Lapostolle emittance value of about 0.19 cm-rad. This value may be an overestimate because of the low energy threshold for light-production in quartz, which makes it difficult to make accurate spot-size measurements when the beam radius is small. To avoid this problem, a spot-size diagnostic using transition radiation in a Kapton target is currently being implemented. This will give a two-dimensional beam image with a 60 ns (the approximate pulse flat-top) gating on the camera.

Using the envelope code LAMDA, we have carried out a series of tests to measure the sensitivity of the minimum spot-size to various machine parameters. The results, shown in Table I, give an indication of the degree of control needed to obtain a small time-averaged spot-size for a particular beam pulse, and that needed for shot-to-shot spot-size reproducibility.

Experiments are currently being conducted on the REX machine to investigate a laser photocathode injector. This has the potential for significantly reducing the intrinsic emittance of the beam. A lower emittance, resulting in a smaller spot-size, would reduce the tolerances in Table I.

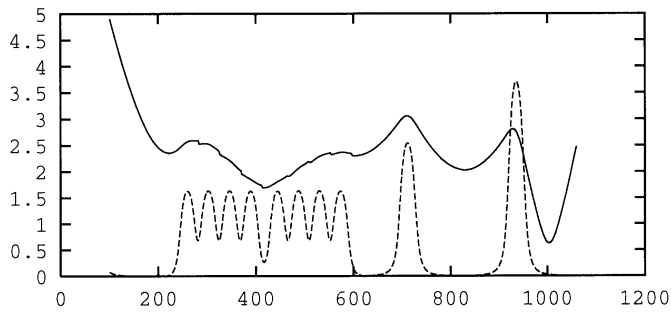


Figure 6. Beam edge radius (cm) vs. z (cm) for final focus magnet current of 370 A, obtained from LAMDA. Axial magnetic field, divided by 300 gauss, is superimposed.

Table I

Percent changes in accelerator parameters which result in 10% change in final-focus spot-size

AK voltage	+20%, -11%
Accelerating gap voltage	+30%, -16%
Cell magnet strength	+17%, -35%
Drift tube magnet	+4.7%, -10%
Final-focus magnet strength	+3.2%, -3.4%
Position of target	+3.5 cm, -8.9 cm

IV. ACKNOWLEDGMENT

This work was performed under the auspices of the U.S. Department of Energy by Los Alamos National Laboratory.

V. REFERENCES

1. J. Boers, Thunderbird Simulations Inc.
2. T. P. Hughes, R. L. Carlson and D. C. Moir, "Calculations for PIXY, ECTOR, REX, ITS and TGX," MRC/ABQ-R-1483, March, 1992.
3. T. P. Hughes, T. C. Genoni, P. W. Allison, R. L. Carlson and D. C. Moir, "Computational Support for ITS and REX," MRC/ABQ-R-1735, April, 1995.
4. T. P. Hughes, R. M. Clark, T. C. Genoni, and M. A. Mostrom, "LAMDA User's Manual and Documentation," MRC/ABQ-R-1428, April, 1993.
5. Paul Allison, "XTR, A New Beam Dynamics Code for DARHT," DARHT Technical Note #50, 13 July 1995.
6. M. Reiser, Phys. Fluids 20, 477 (1977).